Viscous Energy Loss in the Presence of Abnormal Aortic Flow

A.J. Barker[1], **P. van Ooij**[1], **K. Bandi**[2], **J. Garcia**[1], **M. Albaghdadi**[3], **P. McCarthy**[2], **R. O. Bonow**[3], **J. Carr**[1], **J. Collins**[1], **C. Malaisrie**[2], and **M. Markl**[1,4]

[1]Department of Radiology, Northwestern University, Chicago IL

[2]Division of Surgery-Cardiac Surgery, Northwestern University, Chicago IL

[3]Division of Cardiology, Northwestern University, Chicago IL

[4]Department of Biomedical Engineering, Northwestern University, Evanston IL

Abstract

Purpose—To present a theoretical basis for noninvasively characterizing *in vivo* fluid-mechanical energy losses, and to apply it in a pilot study of patients known to express abnormal aortic flow patterns.

Methods—4D flow MRI was used to characterize laminar viscous energy losses in the aorta of normal controls (n=12, age=37±10), patients with aortic dilation (n=16, age=52±8), and patients with aortic valve stenosis matched for age and aortic size (n=14, age=46±15), using a relationship between the 3D velocity field and viscous energy dissipation.

Results—Viscous energy loss was significantly elevated in the thoracic aorta for patients with dilated aorta (3.6±1.3 mW, p=0.024) and patients with aortic stenosis (14.3±8.2 mW, p<0.001) compared to healthy volunteers (2.3±0.9 mW). The same pattern of significant differences were seen in the ascending aorta, where viscous energy losses in patients with dilated aortas (2.2±1.1 mW, p=0.021) and patients with aortic stenosis (10.9±6.8 mW, p<0.001) were elevated compared to healthy volunteers (1.2±0.6 mW).

Conclusion—This technique provides a capability to quantify the contribution of abnormal laminar blood flow to increased ventricular afterload. In this pilot study, viscous energy loss in patient cohorts was significantly elevated and indicates that cardiac afterload is increased due to abnormal flow.

INTRODUCTION

Aortic valve stenosis and insufficiency, whether congenital or acquired, are cardiac valvular lesions that may lead to left ventricular (LV) dysfunction, heart failure, and death. These

Corresponding author: Alex J Barker, Ph.D., Department of Radiology, Northwestern University, 737 N. Michigan Ave, Suite 1600, Chicago, IL 60611, phone: +1 312-926-2736, fax: +1 312-926-5991, alex.barker@northwestern.edu.

lesions increase LV pressure or volume overload, and often result in drastic alterations of post-valvular 3D blood flow patterns (1,2). It is also known that patients with a dilated ascending aorta, but physiologically normal aortic valves, exhibit alterations in 3D aortic blood flow patterns such as enhanced helix or vortex flow. In these cases, the implication for disease progression or ventricular loading is poorly understood (3,4). In cases where patent alterations of ascending aorta flow are present, such as valve disease, the current American Society of Echocardiography (ASE) and American College of Cardiology/American Heart Association (ACC/AHA) standard-of-care guidelines assess disease severity based on simplified measurements local to the valve, such as peak velocity, effective orifice area, regurgitant volume, aortic diameter and transvalvular pressure gradient (5,6). However, it is known that patients with similar degrees of aortic and valvular lesion severity, as assessed by conventional modalities and current guideline metrics, can exhibit radically divergent clinical presentations and outcomes - implying incomplete disease characterization (7–9).

Functional assessment and risk-stratification may thus benefit from a robust methodology capable of quantifying the energetic load placed on the left ventricle due to the presence of altered aortic flow patterns caused by aortic valve abnormalities or dilatation (10). The gold standard for measuring LV load associated with aortic-valve pressure gradient and energy losses is invasive cardiac catheterization. However, catheterization of subjects to compute pressure loss has 2 primary disadvantages: 1) the risk inherent to invasive procedures, 2) potential error due to pressure recovery (8,11). These disadvantages have driven a longstanding effort to develop noninvasive methods that employ cardiac imaging, computational models, or a combination of both (12,13). In this context, 4D flow MRI (time-resolved 3D phase-contrast MRI with all principal velocity directions encoded) has gained increasing importance as it provides the full *in vivo* time-resolved 3D velocity field in the entire aorta. Recently, the estimation of turbulent kinetic energy (TKE) based on 4D flow MRI data has been proposed to non-invasively detect regions of elevated flow turbulence associated with aortic disease such as valve stenosis or coarctation (14). While studies have shown that TKE is sensitive to detect and quantify the presence of regional turbulence, the effect of regions of abnormal or complex non-turbulent flow (such as vortex formation or helical flow), which have been described in numerous previous studies (3,4,15,16), are not captured by this technique.

The aim of this study was therefore to develop and apply a method capable of estimating viscous energy loss, a parameter which can be directly calculated from the *in vivo* 4D flow MRI velocity data. We hypothesize that assessment of viscous energy loss can quantify differences in energetic losses in patients with aortic dilation and aortic valve disease and may thus be a promising candidate to quantify LV loading. This work presents a theoretical basis for the use of 4D flow MRI to characterize *in vivo* energy loss and applies the technique in a pilot study of patients with aortic dilation alone (dilation-only group, n=16) and patients with aortic dilation and aortic valve stenosis (dilated/stenotic group, n=14) as compared to normal controls (n=12).

THEORY

Mechanical Energy and Pressure Recovery

Energy exchange between mechanical energy, i.e. kinetic and potential energy, is ideally conserved. In the case of idealized blood flow across the aortic valve, an increase in blood velocity across the aortic valve plane (i.e. increased kinetic energy) corresponds to a decrease in pressure (decreased potential energy). This concept is important to understand pressure recovery, where an observed transvalvular pressure gradient does not wholly represent permanent pressure loss. Instead, a portion of the pressure loss can be recovered downstream by the conversion of kinetic energy to potential energy (an exchange characterized by the partial recovery of static pressure)(10,17).

Non-idealized Flow and Energy

For non-idealized flow (where mechanical energy is not conserved), kinetic and potential energy are also partially converted to acoustic and thermal energy (due to friction, viscosity, and turbulence), which represents a permanent, unrecoverable loss to the usable mechanical energy of the system (10,18). The left ventricle will experience these mechanical energy losses as an increase in cardiac afterload and therefore stress on the myocardium. In simpler terms, in order to maintain the same net blood flow in a condition where irreversible energy losses increase, the load the heart must contract against will increase (i.e. afterload will increase). For this reason, irreversible pressure loss in post-stenotic flow (as a proxy for total mechanical energy loss) is widely used as a hemodynamic marker of aortic stenosis severity. The method of choice for non-invasive assessment of severity is the approximation of maximum transvalvular pressure gradient (TPG$_{max}$) using echocardiography. The TPG$_{max}$ is estimated by simplified Bernoulli equation (6), where the peak velocity in the aortic valve vena contracta region (v_{VC}) is assumed to be much greater than the velocity in the LV outflow tract (LVOT). Once viscous losses and acceleration terms are assumed to be negligible (i.e. flow is assumed invicsid and steady), the simplified Bernoulli relation is expressed as TPG$_{max} = 4(v_{VC})^2$. However, this relationship is known to overestimate the net transvalvular pressure gradient as measured by invasive catheterization (TPG$_{net}$) (8,10,19). The primary reason for this phenomenon is the sudden contraction and expansion of the outflow tract shape, which causes fluid mechanical losses due to non-idealized flow, but also energy transfer and the phenomenon of pressure recovery. Others have proposed alternative methods to account for the contribution of the geometric factors that contribute to the resulting flow patterns and irreversible pressure loss (20). For example Garcia et al. have proposed the following modification to the Bernoulli equation, which attempts to account for the pressure loss coefficient associated with post-valvular geometric effects:

$$TPG_{net} = 4\nu_{VC}^2 \left(1 - \frac{EOA}{MAA}\right)^2, \quad [1]$$

where the ratio of the effective orifice area (EOA) to the mid-ascending aorta area (MAA) is taken into consideration. This has been shown to have a better correlation with simultaneous invasive catheterization measurements in the left ventricle and ascending aorta (17). However, care must be taken to avoid error due to EOA measurement, the determination of

peak velocity, and the assumptions involving a circular EOA and aorta area. In addition, neither TPG$_{max}$ nor TPG$_{net}$ provide a direct estimate of LV afterload related to the viscous portion of the pressure loss.

Viscous Energy Loss Calculation

Interestingly, non-turbulent energy losses can be non-invasively calculated and visualized using the concept of viscous dissipation (Φ_v). This concept is fundamentally different from the Bernoulli equation in that it does not assume inviscid flow. If the full three-directional fluid velocity field ($\mathbf{v}$) in a domain of interest is known, Φ_v can be computed using a reformulation of the viscous portion of the incompressible Navier-Stokes energy equations, i.e.:

$$\phi_\nu = \frac{1}{2}\sum_i \sum_j \left[\left(\frac{\partial \nu_i}{\partial x_j} + \frac{\partial \nu_j}{\partial x_i} \right) - \frac{2}{3}(\nabla \cdot \boldsymbol{\nu})\delta_{ij} \right]^2 \; where \; \begin{matrix} \delta_{ij}=1 \, for \, i=j \\ \delta_{ij}=0 \, for \, i \neq j \end{matrix} \quad [2]$$

in which i and j are the principal directions x, y, z (18). Thus, Φ_v results in a map of the viscous dissipation on a voxel by voxel basis. Ultimately, the rate of energy loss in a volume of interest (i.e. power in Watts) at a given moment in the cardiac cycle can be found with the product of the dynamic viscosity of blood (μ) and the integral of the the voxel-wise dissipation map:

$$E'_L = \mu \sum_{i=1}^{num \; voxels} \phi_\nu V_i, \quad [3]$$

where and V_i is the voxel volume. E_L' can be integrated over time to obtain the net energy loss in Joules (i.e. E_L).

As shown previously, 4D flow MRI can be employed to quantify the three-directional fluid velocity field *in vivo* with full volumetric coverage of the thoracic aorta (21). The 3D velocity field in a region of interest can thus be used to provide the necessary data to compute Φ_v, the rate of instantaneous viscous energy loss E_L' (e.g. instantaneous power loss), and upon integrating over the cardiac cycle, the net viscous energy loss over time (E_L).

METHODS

Subject Enrollment

To investigate the impact of aortic valve stenosis and dilation on aortic hemodynamics, 3 subject groups were retrospectively constructed from a database of 134 subjects who underwent a 4D flow MRI between November 2011 and December 2012. The cohorts were composed of: 1) healthy volunteers with normal aortic valve function and thoracic aorta geometry (n=12), 2) patients with normal aortic valve function referred for MRI to evaluate aortic dilatation (dilation-only group, n=16), and 3) patients referred for MRI to evaluate aortic stenosis severity and found to have aortic dilation (dilated/stenotic group, n=14). Cohorts were matched for age and patient cohorts were matched for aortic diameter. Aortic dilation was defined as a sinus of valsalva (SOV) or mid-ascending aorta (MAA) diameter > 4.0 cm. Stenosis patients were categorized according to the absolute systolic peak velocities

in the LVOT, as is recommended by echocardiography guidelines (mild: 2.9 m/s, moderate: 3–4 m/s, severe: >4m/s) (6). Bicuspid aortic valve (BAV) was present in 5 of the 16 aortic dilation-only patients and 7 of the 14 stenosis patients. Demographics are summarized in Table 1. The study was approved by the Institutional Review Board of Northwestern University (IRB). Informed consent was obtained from all healthy volunteers. Patients were included in accordance with an IRB protocol which permitted retrospective chart review.

MR Imaging

All participants underwent a standard-of-care thoracic cardiovascular MRI at 1.5T (Magnetom Espree or Avanto, Siemens Medical Systems, Germany). The MRI exam included ECG gated time-resolved (CINE) cardiac MRI for the evaluation of cardiac function and valve morphology, as well as contrast enhanced MR angiography (CE-MRA) for the quantification of aortic dimensions. For the assessment of aortic blood flow, time-resolved 3D phase-contrast MRI with three-directional velocity encoding (4D flow MRI) was obtained in a sagittal oblique 3D volume covering the thoracic aorta using prospective ECG gating during free breathing with a respiratory navigator placed on the lung-liver interface. Pulse sequence parameters for the 4D flow scan were as follows: TE/TR=2.3–3.4/4.8–6.6 ms, flip angle α=7–15°, temporal resolution=38.4–52.5 ms; field of view = 340–400×200–300 mm, spatial resolution = 1.8–2.1×1.8–2.1×2.0–2.8 mm^3. Velocity sensitivity was adjusted to minimize velocity aliasing (venc = 1.5–4.0 m/s).

Data Analysis

A schematic of the data analysis strategy is shown in Fig. 1. 4D flow MRI data were pre-processed to correct for eddy currents and Maxwell terms. If present, velocity aliasing was semi-automatically corrected by applying a previously described automated correction (22). Subsequently, all data were reviewed and voxels with persistent velocity aliasing were manually identified and corrected. For each subject, flow-time curves and peak velocities at the level of the aortic valve vena contracta were extracted from the 4D flow data to identify peak systole (defined as the peak flow rate) and peak systolic velocity (v_{VC}, as found from the Euclidean norm of the MRI velocity vectors). Next, the signal intensity of the 4D flow magnitude data was used to define a level-set 3D segmentation of the thoracic aorta lumen (vmtk v1.0.0, Orobix, Bergamo, Italy) at peak systole for each subject (23). For each thoracic aorta segmentation, a 3D subregion was created which corresponded to the ascending aorta portion of the original segmentation (the region from the aortic valve annulus to the first brachiocephalic branch, as shown in Fig. 2, dashed region) using ImageJ (v1.45s, NIH, Bethesda, USA). Both 3D segmentations were then used to mask the peak systolic 3D velocity field obtained from the 4D flow MRI data. A 3D 3×3 median filter was applied to the masked velocity field to mitigate noise. In order to facilitate characterization of internal flow features such as jets, vortices, and helices, the dissipation at near wall voxels was not calculated (masked domain was set to 'NaN', i.e. 'not a number'). The energy loss rate (i.e. E_L') at the peak flow systole time point was then subsequently calculated using Eq. 3 in both the entire thoracic aorta and the ascending aorta (viscosity was assumed Newtonian at 3.2 cP). For the purpose of illustrating the energy loss experienced along two

different flow paths; rather than using Eq 3, the viscous dissipation (Φ_v) was integrated along the paths shown in Fig 1b, assuming a steady flow field defined at peak flow systole.

Observer Variability

To test the impact of the interobserver variability in the semi-automatically generated 3D volume of the thoracic and ascending aorta, the 3D segmentation process was performed by two independent observers for 30 subjects (10 controls, 10 aortic dilation-only patients, and 10 stenosis patients). For both observers, systolic energy loss was independently calculated based on the 3D masks of the peak systolic 3D velocity field.

Statistical Analysis

All data are expressed as mean ± standard deviation. Intergroup comparisons of mean values were analyzed with a Wilcoxon rank-sum test. A P value less than 0.05 was considered statistically significant. Agreement between observers was assessed by a Bland-Altman comparison of peak systolic energy loss. From these data, the mean difference and limits of agreement (±1.96 SD) were calculated. To identify relationships between viscous energy loss and measures of disease severity (mid-ascending aortic diameter, transvalvular pressure gradient), univariate and multivariate linear regressions were performed and the coefficient of determination (r^2) was calculated; a correlation was considered significant if $P < 0.05$.

RESULTS

Viscous Energy Loss in the Aorta

After age-matching and cohort selection, 42 subjects were included in the final study population. Of the patients referred for stenosis, all were found to have mild (n=3), moderate (n=5) or severe (n=6) stenosis. Of those referred for dilation, one patient was found to have significant stenosis (as determined by peak velocity) and re-categorized in the aortic stenosis group. 4D flow MRI, aortic 3D segmentation, and calculation of viscous energy loss was successfully completed in all 42 subjects. Fig. 2 shows representative examples of the resulting energy loss maps in the thoracic aorta of a normal healthy volunteer compared to a patient with severe aortic stenosis. Note that regions known to exhibit flow separation ('*'), flow jet impingement (**, white arrow), and spatially isolated high peak velocities ('**', black arrow) resulted in elevated energy loss due to viscous effects. The high velocity flow jet (v_{VC}=4 m/s) and the flow jet wall impingement region in the patient with tricuspid leaflet anatomy and aortic stenosis led to a 20-fold increase in ascending aortic energy loss. This is indicative of a reduction in the available mechanical energy to the system and thus elevated ventricular loading. Noticeably, the regions of high energy loss were not isolated to the jet region corresponding to the stenotic aortic valve, but also present in the region where the flow jet impinged on the anterior aortic wall. Additionally, it is notable that local regions known to exhibit flow separation and vortex formation in healthy subjects (Fig. 2, '*') were also co-located with elevated energy loss.

The cumulative result of energy loss quantification for all subjects is summarized in Fig. 3. Viscous energy loss was statistically elevated in the thoracic aorta for patients with normal valves and dilated aorta (E_L'=3.6±1.3 mW, P=0.024) and patients with aortic stenosis

(E_L'=14.3±8.2 mW, P<0.001) compared to healthy volunteers (E_L'=2.3±0.9 mW). The same relative significant differences were seen in the ascending aorta, where viscous energy losses in patients with dilated aortas (E_L'=2.2±1.1 mW, P=0.021) and patients with aortic stenosis (E_L'=10.9±6.8 mW, P<0.001) were elevated compared to healthy volunteers (E_L'=1.2±0.6 mW). On average, the ascending aorta accounted for 71% of the overall energy loss in the thoracic aorta.

Bland-Altman analysis for all cohorts (Fig. 4) demonstrated low interobserver variability for E_L', with a mean bias of 0.068 mW and limits of agreement of ±1.75 mW (or a mean of 7% for the measured values). Notably, the limits of agreement were ±0.61 mW (or a mean of 8% for the measured values) when the stenotic cohort was excluded.

Impact of Deranged Flow on Viscous Energy Loss

The use of viscous energy loss to quantify a relative increase in energy cost for abnormal compared to normal flow is illustrated in Fig. 1 using an example BAV patient with mild stenosis and SOV and MAA diameters of 4.7 and 4.5 cm, respectively. In this example, two 3D systolic streamlines depict two substantially different flow pathways passing the same vascular landmarks in the thoracic aorta of this patient (Fig. 1a). While flow originating near the anterior region of the aortic valve travels along a helix pattern in the ascending aorta, blood from the posterior region of the valve exhibits a more direct flow path. Fig. 1b illustrates the considerably higher energetic cost of the abnormal helix flow compared to the direct route (180% increase in E_L' when reaching the proximal descending aorta, point 3 in Fig. 1b).

Viscous Energy Loss and Disease Severity

Fig. 5 and 6 show the correlation of aortic energy loss with disease severity as expressed by the pressure gradient across the aortic valve and by the extent of aortic dilatation (mid-ascending aortic diameter, MAA), respectively. For all 42 subjects, univariate regression analysis revealed a strong and significant correlation (r^2=0.91, P<0.001) to increased energy loss with the TPG_{net}, as shown in Fig. 5. This correlation was slightly better than that found for TPG_{max} (r^2=0.86, P<0.001). For subjects with unobstructed aortic valves (healthy volunteers and patients with dilated aorta, n=28) there was a moderately significant correlation (r^2=0.55, P<0.001) between increased aortic dilation and elevated energy loss (Fig. 6). For patients with aortic valve stenosis, no correlation with aortic diameter was found (r^2=0.14, P=0.19) (10,20). Multivariate regression analysis of all cohorts found that transvalvular pressure gradient was significantly correlated to energy loss (P < 0.001) and no significance existed for aortic diameter (P = 0.23).

DISCUSSION

In this study, the theory and novel *in vivo* assessment of 4D flow MRI-based viscous energy loss was introduced to quantify altered 3D flow characteristics in healthy subjects and 2 patient groups (those with dilated ascending aortas and those with aortic valve stenosis and concomitant dilation). These pathologies are known to exhibit complex 3D flow abnormalities such as helix formation, vortex formation, and flow jets, which will ultimately

increase energetic losses within the ascending aorta (10,24). Our findings demonstrate the sensitivity of this viscous energy loss estimation technique in detecting differences in energetic losses between patient cohorts (Fig. 2). Moreover, a strong correlation with traditional measures of disease severity (e.g mid-ascending aortic diameter and transvalvular pressure gradient) exists. The mechanism of viscous energy loss presented here quantifies irreversible, non-turbulent energy loss, and thus is a metric indicative of increased LV workload. For this reason, the technique may prove useful as a clinical marker for patient stratification, especially in the challenging cases of low-flow, low gradient aortic stenosis where aortic size and stiffness are known to significantly impact LV function (e.g. ventriculo-arterial coupling) (8).

Previous *in-vitro* experimental studies have demonstrated the agreement of MRI-derived energy loss with computational fluid dynamic models (25). In addition, the marked elevation of energy loss in patients with aortic stenosis agrees well with large pressure gradients known to exist for this patient cohort. The large spread in measured E_L' values may be representative of the spectrum of aortic stenosis in the study cohort (Table 1, Fig. 3). In this respect, the degree of stenosis by the simplified Bernoulli equation (TPG_{max}) was found to significantly correlate with E_L' (r^2=0.86, P<0.001). However, it should be noted that perfect correlation is not expected, given that measurement of pressure gradient by Bernoulli's equation is confounded by idealized flow assumptions and the lack of accounting for pressure recovery. This is known to result in misclassification when using the pressure gradient for aortic stenosis severity assessment (19). Support for this theory is demonstrated by the increase in correlation quality between the TPG_{max} calculated by the simplified Bernoulli equation and the EOA-corrected Bernoulli TPG_{net} proposed by Garcia et al. (r^2=0.91, P<0.001, Fig. 5) (17). Nonetheless, it should be noted that even the corrected equation uses a number of idealized flow assumptions that do not take into account converging flow, complex flow (helical and vortical flow features) and flow jet/lumen wall impingement. As mentioned, the equation is also susceptible to error related to EOA measurement, peak velocity, and the assumption of a circular orifice and aorta. These challenges highlight various advantages of the viscous dissipation technique, i.e.: 1) invasive pressure measurements are avoided, 2) the technique is not susceptible to errors caused by pressure recovery, 3) regions of complex flow are accounted for, and 4) regions of permanent energy loss are easily visualized.

In order to understand the impact of ascending aorta size on the energy loss measurements, an ascending aorta subregion was isolated from the thoracic aorta. In agreement with previous studies that found helical and vortical flow is positively correlated with ascending aorta diameter (3,4), our findings demonstrated a correlation of increased energy loss with aortic dilation. The idealized case in Fig. 1 illustrates the mechanism by which helical features increase the overall energy loss of the system; however for the stenosis group, flow changes induced by the rapid contraction, obstruction, and expansion of the outflow tract geometry appear to far exceed the contribution of helical and vortical flow to overall energy loss. Heinrich et al. have previously reported the increased energy loss due to these geometric inflow and outflow effects and that they increase rapidly with increasing degrees of valve obstruction and degree of inflow/outflow tract shape changes (20). Thus, the

correlation of MAA diameter to E_L' was strongest for the control and dilation-only cohorts (Fig. 6). In addition, it is observed that the majority of dissipation is occurring in the ascending aorta, as is supported by the fact that for all subjects 71% of total energy loss in the thoracic aorta was contained in the ascending aorta region (Fig. 3).

The resting power output of the heart can be approximated by taking the product of the average cardiac output and the pressure imparted by the left ventricle. Further simplified, E_{heart}'=CO*MAP, where CO is the average cardiac output (~5 L/min) and MAP is the mean arterial pressure (~80 mmHg). Thus, we estimate the resting cardiac power output of the heart to be on the order of ~1 W. In absolute terms, E_L' as computed using the methods presented here, would be ~0.2–3% of the overall output of the heart. However, we stress that the methods we have presented for the estimation of energy loss associated with abnormal flow did not take into account: 1) energy lost over the entire cardiac cycle, 2) viscous dissipation associated with the vessel wall, and 3) effects due to turbulence. All of these items can be addressed in future studies. For example, it is well understood that rapid geometric changes and regions of high velocity gradients (such as those observed in our aortic valve stenosis patients) are often accompanied by wall regions with high viscous dissipation and regions of turbulence (characterized by random temporal and spatial velocities fluctuations) (26,27). The irregular and rapid fluctuations due to turbulence are not directly represented in the three-directional blood flow velocities in each imaging voxel as measured by the 4D flow MRI technique. However, as shown by Dyverfeldt et al., the magnitude of the signal can be used to measure the standard deviation of the velocity within a voxel, which is related to the turbulent kinetic energy (TKE), a direction independent measure of turbulence intensity (14). The combination of the velocity field and turbulent kinetic energy can give a visualization of disturbed flow. A number of recent studies have shown the value and sensitivity of 4D flow MRI based TKE mapping to detect elevated values of turbulent kinetic energy caused by valvular obstruction or other abnormalities (12,28). In addition, blood flow patterns and turbulence intensity downstream from a prosthetic heart valve have been found to be dependent on the specific valve design (29). Since our study did not account for viscous losses due to wall effects or turbulent flow, we speculate that the fluid energy lost in the setting of a stenotic valve, which is also known to be associated with turbulent flow, is elevated beyond the solely viscous values reported here. We postulate that viscous energy loss and turbulent energy loss are correlated. Future studies are needed to investigate the contribution of abnormal aortic flow patterns to all viscous energy losses and TKE to fully understand the impact of aortic disease on net energy loss and ventricular loading. Nevertheless, the findings in our study demonstrate the contribution of jetting, helicity, and vorticity to the viscous dissipation and the overall energy loss in the ascending aorta. These energy losses were significantly elevated in both patient cohorts as compared to controls. Energy loss in patients with aortic dilation alone was slightly elevated whereas energy losses in patients with aortic stenosis were increased by more than an order of magnitude compared to controls.

Viscous energy loss alone may be a promising new metric of aortic hemodynamics to characterize the functional consequences of altered aortic 3D blood flow patterns. Although the full three-directional velocity field is needed to estimate viscous energy loss, the 3D

segmentation of a vascular region of interest provides the opportunity to calculate a single number (E_L') than can be easily communicated to clinicians. In addition and if desired, energy loss maps can easily be generated which can provide insights into the spatial localization of hot spots for energy loss. Future studies are needed to analyze the diagnostic value of such maps as they correlate to the development and progression of aortic disease, for example, the progressive regional aortic dilation at the location of flow impingement zones as shown in Fig. 2 ('**').

Limitations

The potential advantages of this technique are tempered by two main challenges, 1) variability introduced by the segmentation step and 2) spatiotemporal resolution. For example, small variations in observer segmentation will introduce variability to the energy loss velocity gradient calculations (Eq. 2). The increase in interobserver variability in the stenosis patients is possibly due to the presence of high velocity outflow jets near the aorta wall, and thus high velocity gradients sensitive to segmentation position. For this reason, segmentation variability was assessed with an interobserver study and found to have a mean limit of agreement of 6% for the energy loss in the stenosis patients (Fig 4). In addition, the current spatiotemporal resolution of 4D flow MRI and the smoothing kernel used for the energy loss quantification may underestimate the magnitude of the laminar component of viscous energy loss and introduce resolution limits to the accuracy of our calculations. Although invasive validation was not performed and no gold standard for *in vivo* viscous energy loss measurement exists, experimental comparison to computational fluid dynamics (CFD) have found agreement between the *in vitro* measurement of mechanical energy loss and the MRI-technique presented here (25). In addition, small lumen diameters (<1 cm) or slow recirculation flow may result in decreased velocity-to-noise ratio or too few pixels available for energy loss estimation. For this reason, we excluded the supra-aortic branches from the calculation domain, where diameters below 1 cm in diameter are common. However, these limitations do not apply to the ascending aorta, a region with large diameters and high systolic flow, where the most important findings of this study occur. Additionally, the limited resolution in our study does not affect the general energy loss distributions or relative differences between the patients and volunteer cohorts.

For the purpose of this initial pilot study, tricuspid and bicuspid aortic valve leaflet morphologies were included in the stenosis group. However, the morphology and leaflet configuration may additionally influence the 3D blood flow patterns and thus the overall energy loss (2). Future studies should investigate these groups independently with more rigorous selection for age-matching than performed here (P=0.14). Furthermore, specific cardiac pathologies were chosen for our study cohorts, which do not cover the entire spectrum of possible disease states. Future studies investigating aortic insufficiency, low flow/low gradient stenosis, and borderline/discrepant cases will help determine the clinical utility of this technique.

CONCLUSION

Increased aortic energy loss measured in the chosen patient cohorts indicates that the left ventricle must work harder to overcome inefficiencies introduced by abnormal aortic flow. Measuring energy loss may prove useful for risk stratification and functional assessment of aortic dilation and aortic stenosis. Longitudinal data collection is ongoing to understand the association of viscous energy loss with clinical outcomes.

Acknowledgments

REFERENCES

1. Briand M, Dumesnil JG, Kadem L, Tongue AG, Rieu R, Garcia D, Pibarot P. Reduced systemic arterial compliance impacts significantly on left ventricular afterload and function in aortic stenosis: implications for diagnosis and treatment. J Am Coll Cardiol. 2005; 46:291–298. [PubMed: 16022957]

2. Barker AJ, Markl M, Burk J, Lorenz R, Bock J, Bauer S, Schulz-Menger J, von Knobelsdorff-Brenkenhoff F. Bicuspid aortic valve is associated with altered wall shear stress in the ascending aorta. Circ Cardiovasc Imaging. 2012; 5:457–466. [PubMed: 22730420]

3. Burk J, Blanke P, Stankovic Z, Barker A, Russe M, Geiger J, Frydrychowicz A, Langer M, Markl M. Evaluation of 3D blood flow patterns and wall shear stress in the normal and dilated thoracic aorta using flow-sensitive 4D CMR. J Cardiovasc Magn Reson. 2012; 14:84. [PubMed: 23237187]

4. Frydrychowicz A, Berger A, Munoz Del Rio A, Russe MF, Bock J, Harloff A, Markl M. Interdependencies of aortic arch secondary flow patterns, geometry, and age analysed by 4-dimensional phase contrast magnetic resonance imaging at 3 Tesla. Eur Radiol. 2012; 22:1122–1130. [PubMed: 22207269]

5. Bonow RO, Carabello BA, Chatterjee K, de Leon AC Jr, Faxon DP, Freed MD, Gaasch WH, Lytle BW, Nishimura RA, O'Gara PT, O'Rourke RA, Otto CM, Shah PM, Shanewise JS. 2008 Focused update incorporated into the ACC/AHA 2006 guidelines for the management of patients with valvular heart disease: a report of the American College of Cardiology/American Heart Association Task Force on Practice Guidelines (Writing Committee to Revise the 1998 Guidelines for the Management of Patients With Valvular Heart Disease): endorsed by the Society of Cardiovascular Anesthesiologists, Society for Cardiovascular Angiography and Interventions, and Society of Thoracic Surgeons. Circulation. 2008; 118:e523–e661. [PubMed: 18820172]

6. Baumgartner H, Hung J, Bermejo J, Chambers JB, Evangelista A, Griffin BP, Iung B, Otto CM, Pellikka PA, Quinones M. Echocardiographic assessment of valve stenosis: EAE/ASE recommendations for clinical practice. J Am Soc Echocardiogr. 2009; 22:1–23. [PubMed: 19130998]

7. Minners J, Allgeier M, Gohlke-Baerwolf C, Kienzle RP, Neumann FJ, Jander N. Inconsistent grading of aortic valve stenosis by current guidelines: haemodynamic studies in patients with apparently normal left ventricular function. Heart. 2010; 96:1463–1468. [PubMed: 20813727]

8. Pibarot P, Dumesnil JG. Improving Assessment of Aortic Stenosis. J Am Coll Cardiol. 2012; 60:169–180. [PubMed: 22789881]

9. Pape LA, Tsai TT, Isselbacher EM, Oh JK, O'Gara PT, Evangelista A, Fattori R, Meinhardt G, Trimarchi S, Bossone E, Suzuki T, Cooper JV, Froehlich JB, Nienaber CA, Eagle KA. Aortic diameter >or = 5.5 cm is not a good predictor of type A aortic dissection: observations from the International Registry of Acute Aortic Dissection (IRAD). Circulation. 2007; 116:1120–1127. [PubMed: 17709637]

10. Akins CW, Travis B, Yoganathan AP. Energy loss for evaluating heart valve performance. J Thorac Cardiovasc Surg. 2008; 136:820–833. [PubMed: 18954618]

11. Omran H, Schmidt H, Hackenbroch M, Illien S, Bernhardt P, von der Recke G, Fimmers R, Flacke S, Layer G, Pohl C, Luderitz B, Schild H, Sommer T. Silent and apparent cerebral embolism after retrograde catheterisation of the aortic valve in valvular stenosis: a prospective, randomised study. Lancet. 2003; 361:1241–1246. [PubMed: 12699950]

12. Dyverfeldt P, Hope MD, Tseng EE, Saloner D. Magnetic resonance measurement of turbulent kinetic energy for the estimation of irreversible pressure loss in aortic stenosis. JACC Cardiovasc Imaging. 2013; 6:64–71. [PubMed: 23328563]

13. Whitehead KK, Pekkan K, Kitajima HD, Paridon SM, Yoganathan AP, Fogel MA. Nonlinear power loss during exercise in single-ventricle patients after the Fontan: insights from computational fluid dynamics. Circulation. 2007; 116:I165–I171. [PubMed: 17846299]

14. Dyverfeldt P, Sigfridsson A, Kvitting JPE, Ebbers T. Quantification of intravoxel velocity standard deviation and turbulence intensity by generalizing phase-contrast MRI. Magn Reson Med. 2006; 56:850–858. [PubMed: 16958074]

15. Hope, MD.; Hope, TA.; Ordovas, K.; Meadows, A.; Saloner, D.; Reddy, GP.; Alley, MT.; Higgins, CB. Clinical Evaluation of Aortic Coarctation with 4D Flow MR Imaging. 16th Annual Meeting of the International Society of Magnetic Resonance in Medicine; Toronto, ON. 2008. p. 1373

16. Reiter G, Reiter U, Kovacs G, Kainz B, Schmidt K, Maier R, Olschewski H, Rienmueller R. Magnetic Resonance Derived 3-Dimensional Blood Flow Patterns in the Main Pulmonary Artery as a Marker of Pulmonary Hypertension and a Measure of Elevated Mean Pulmonary Arterial Pressure. Circ Cardiovasc Imaging. 2008; 1:23–30. [PubMed: 19808511]

17. Garcia D, Pibarot P, Dumesnil JG, Sakr F, Durand LG. Assessment of aortic valve stenosis severity - A new index based on the energy loss concept. Circulation. 2000; 101:765–771. [PubMed: 10683350]

18. Bird, RB.; Stewart, WE.; Lightfoot, EN. Transport Phenomena. New York: John Wiley and Sons, Inc.; 1960.

19. Bahlmann E, Cramariuc D, Gerdts E, Gohlke-Baerwolf C, Nienaber CA, Eriksen E, Wachtell K, Chambers J, Kuck KH, Ray S. Impact of Pressure Recovery on Echocardiographic Assessment of Asymptomatic Aortic Stenosis: A SEAS Substudy. JACC Cardiovasc Imaging. 2010; 3:555–562. [PubMed: 20541709]

20. Heinrich RS, Marcus RH, Ensley AE, Gibson DE, Yoganathan AP. Valve orifice area alone is an insufficient index of aortic stenosis severity: effects of the proximal and distal geometry on transaortic energy loss. J Heart Valve Dis. 1999; 8:509–515. [PubMed: 10517392]

21. Markl M, Harloff A, Bley TA, Zaitsev M, Jung B, Weigang E, Langer M, Hennig J, Frydrychowicz A. Time-resolved 3D MR velocity mapping at 3T: Improved navigator-gated assessment of vascular anatomy and blood flow. J Magn Reson Imaging. 2007; 25:824–831. [PubMed: 17345635]

22. Bock, J.; Kreher, BW.; Hennig, J.; Markl, M. Optimized pre-processing of time-resolved 2D and 3D phase contrast MRI data. Proceedings of the 15th Scientific Meeting of the ISMRM; Berlin, Germany. 2007. p. 3138

23. Antiga L, Piccinelli M, Botti L, Ene-Iordache B, Remuzzi A, Steinman DA. An image-based modeling framework for patient-specific computational hemodynamics. Med Biol Eng Comput. 2008; 46:1097–1112. [PubMed: 19002516]

24. Yap CH, Dasi LP, Yoganathan AP. Dynamic hemodynamic energy loss in normal and stenosed aortic valves. J Biomech Eng. 2010; 132:021005. [PubMed: 20370242]

25. Venkatachari AK, Halliburton SS, Setser RM, White RD, Chatzimavroudis GP. Noninvasive quantification of fluid mechanical energy losses in the total cavopulmonary connection with magnetic resonance phase velocity mapping. Magn Reson Imaging. 2007; 25:101–109. [PubMed: 17222721]

26. Barker AJ, Staehle F, Bock J, Jung BA, Markl M. Analysis of Complex Cardiovascular Flow using Three-Component Acceleration-Encoded MRI. Magn Reson Med. 2012; 67:50–61. [PubMed: 21590722]

27. Saikrishnan N, Yap CH, Milligan NC, Vasilyev NV, Yoganathan AP. In vitro characterization of bicuspid aortic valve hemodynamics using particle image velocimetry. Ann Biomed Eng. 2012; 40:1760–1775. [PubMed: 22318396]

28. Dyverfeldt P, Gardhagen R, Sigfridsson A, Karlsson M, Ebbers T. On MRI turbulence quantification. Magn Reson Imaging. 2009; 27:913–922. [PubMed: 19525079]

29. Kvitting JP, Dyverfeldt P, Sigfridsson A, Franzen S, Wigstrom L, Bolger AF, Ebbers T. In vitro assessment of flow patterns and turbulence intensity in prosthetic heart valves using generalized phase-contrast MRI. J Magn Reson Imaging. 2010; 31:1075–1080. [PubMed: 20432341]
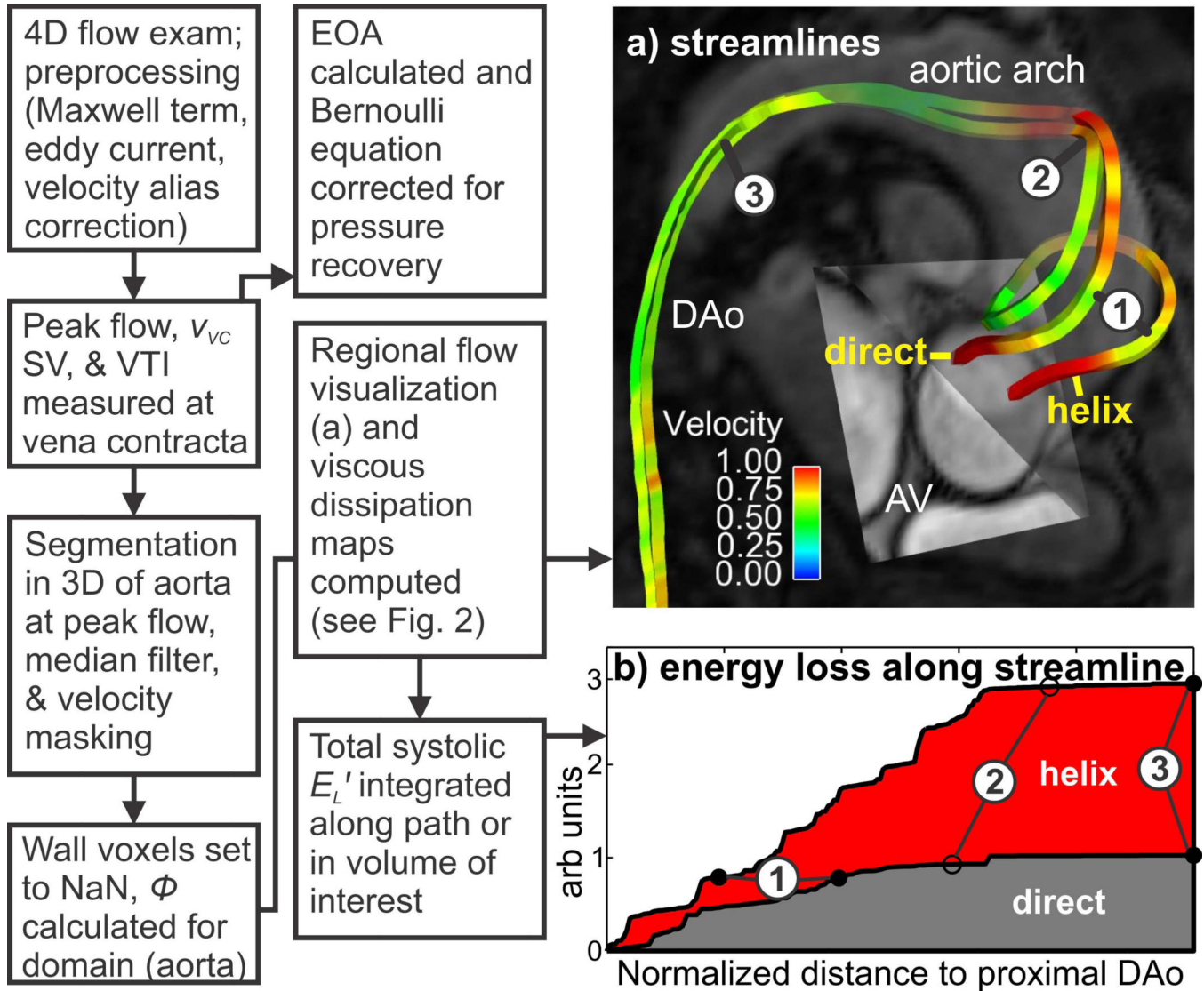
Fig. 1.
Schematic illustrating the energy loss workflow to quantify the effect of **(a)** two different idealized flow paths on **(b)** the viscous energy loss integrated along these paths (note: for the purpose of demonstration, steady flow using the velocity field at peak flow systole was assumed). The 'helix' path exhibits greater energy loss compared to a particle traveling along the 'direct' path (when traversing vascular landmark 1 to 2). A similar workflow was used to integrate the voxel-wise energy loss in the entire aorta volume in order to obtain net energy loss at a single time point. v_{VC}: peak velocity at the vena contracta, SV: stroke volume, VTI: velocity time integral, EOA: effective orifice area, E_L': systolic energy loss, AV: aortic valve, DAo: descending aorta.
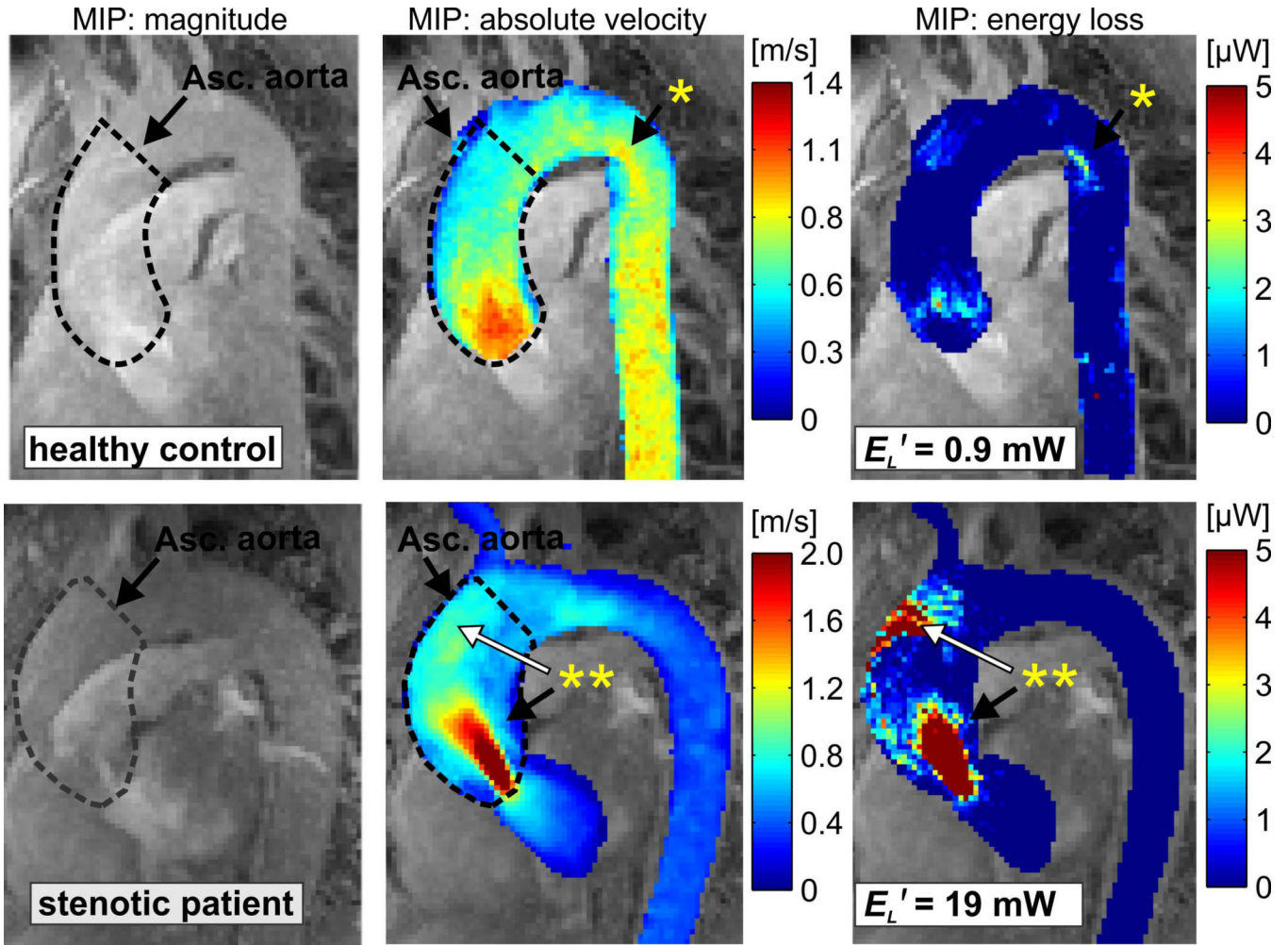
Fig. 2.
Left anterior oblique maximum intensity projection (MIP) of the peak systolic 3D magnitude images, systolic 3D velocity field, and systolic viscous dissipation in the thoracic aorta of a healthy control (peak systolic velocity = 1.2 m/s, top) and a patient with borderline severe stenosis (peak systolic velocity of 4.0 m/s, bottom). The dashed lines indicate the 3D segmentation of the ascending aorta. Known areas of flow separation exhibited of evidence of moderate energy loss (*). Regionally high velocities (**, black arrow) resulted in substantially elevated energy loss. Flow jet impingement at the aortic wall (**, white arrow) was also co-located with a region of substantial energy loss. E_L': cumulative peak systolic energy loss in the ascending aorta.
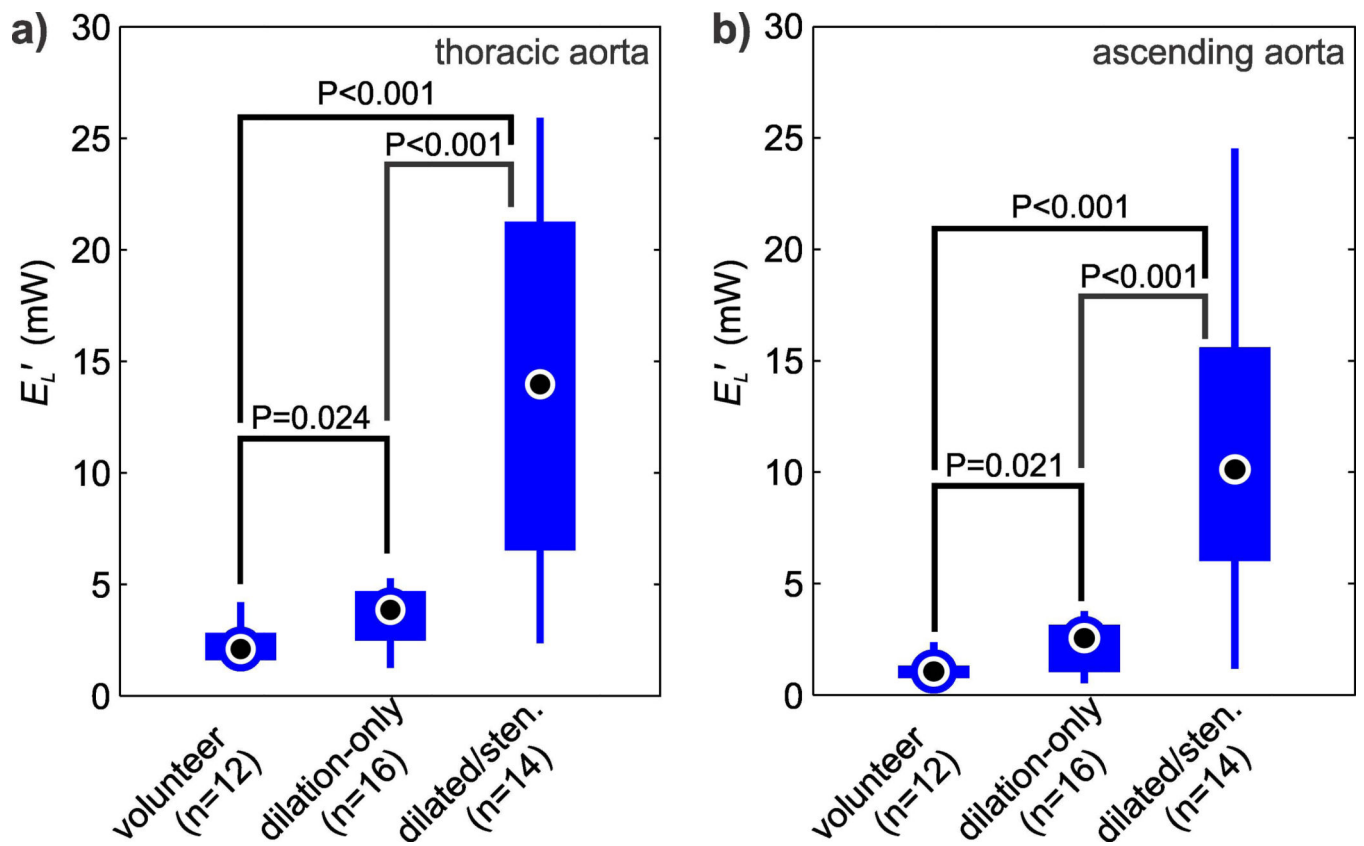
Fig. 3.
Comparison of peak systolic energy loss (E_L') in: **(a)** the thoracic aorta of normal volunteers, dilation-only patients, and in dilated/stenosis patients. **(b)** E_L' in the ascending aorta of the same cohorts. The individual box plots show the distribution of energy loss in each cohort (circle = mean, box = 25%–75% quartiles, whiskers = extrema).
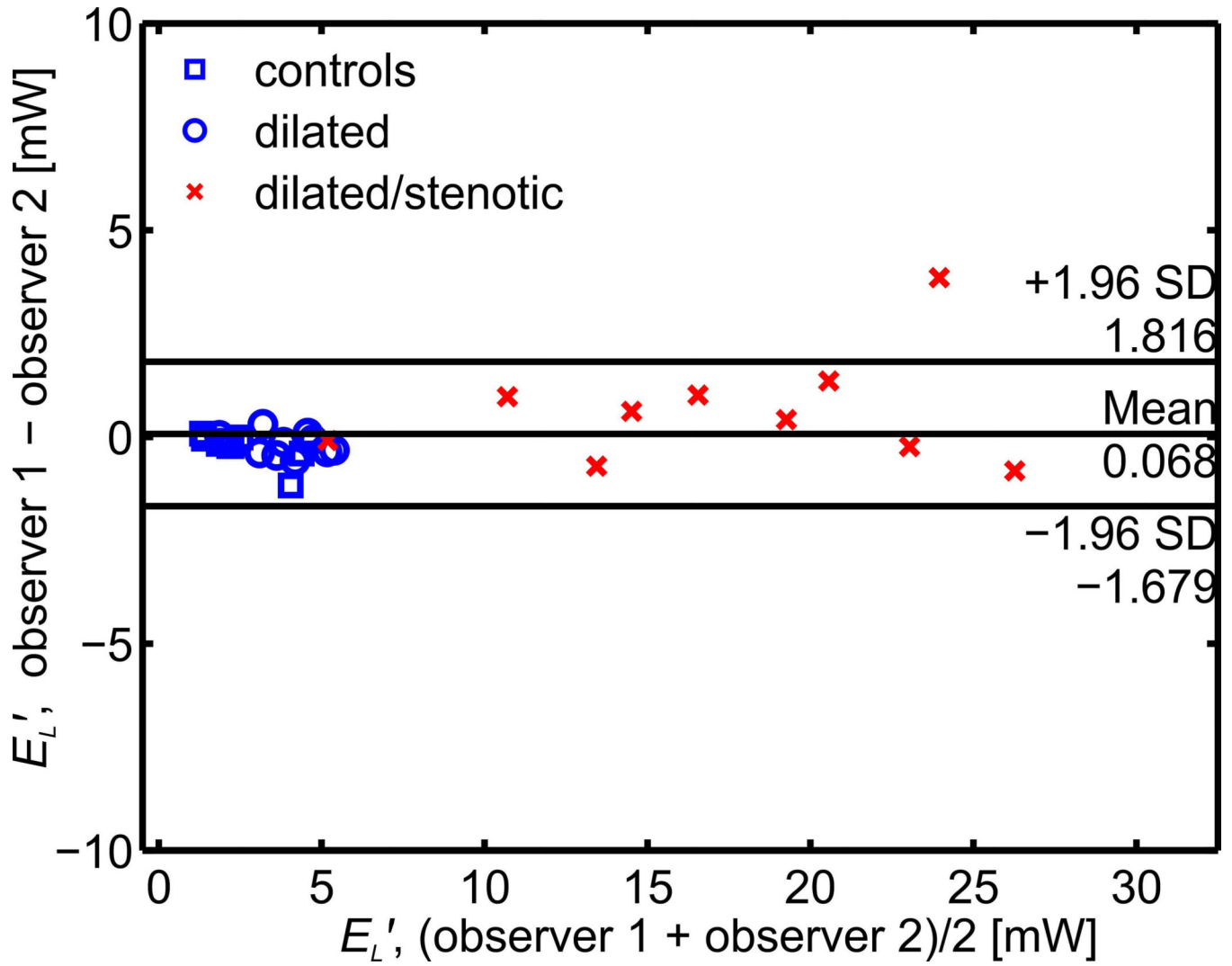
Fig. 4.
Interobserver Bland Altman analysis for the peak systolic energy loss (E_L') calculation in a subgroup of 30 subjects.
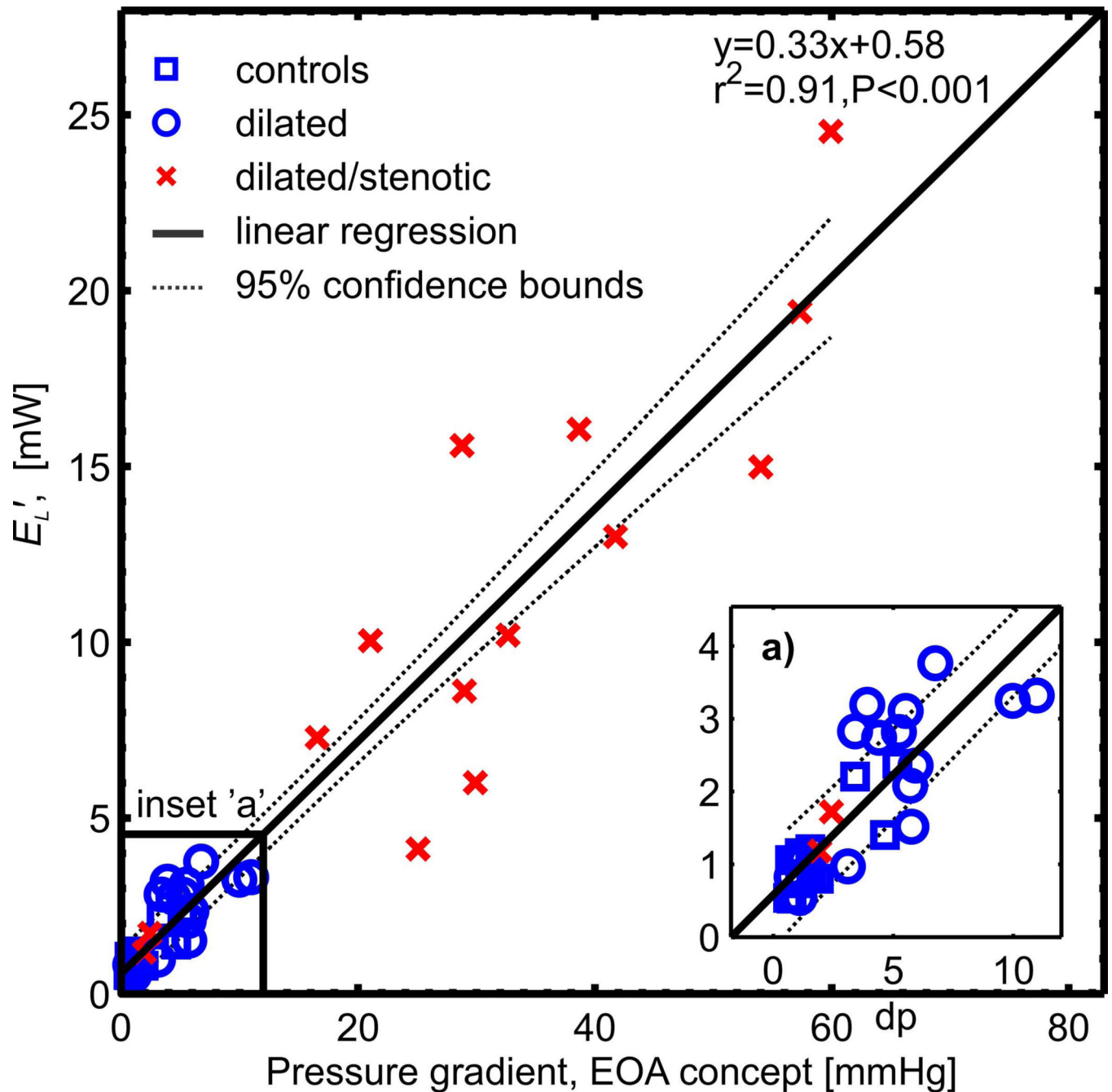
Fig. 5.
Systolic energy loss (E_L') in the ascending aorta of healthy, dilation-only, and dilated/stenotic aorta cohorts as compared to the net transvalvular pressure gradient (TPG$_{net}$, Eq. 1), as calculated by the Bernoulli equation modified to account for pressure recovery effects (17). This correlation was slightly better than the correlation of E_L' to TPG$_{max}$ (r^2=0.86, P<0.001).
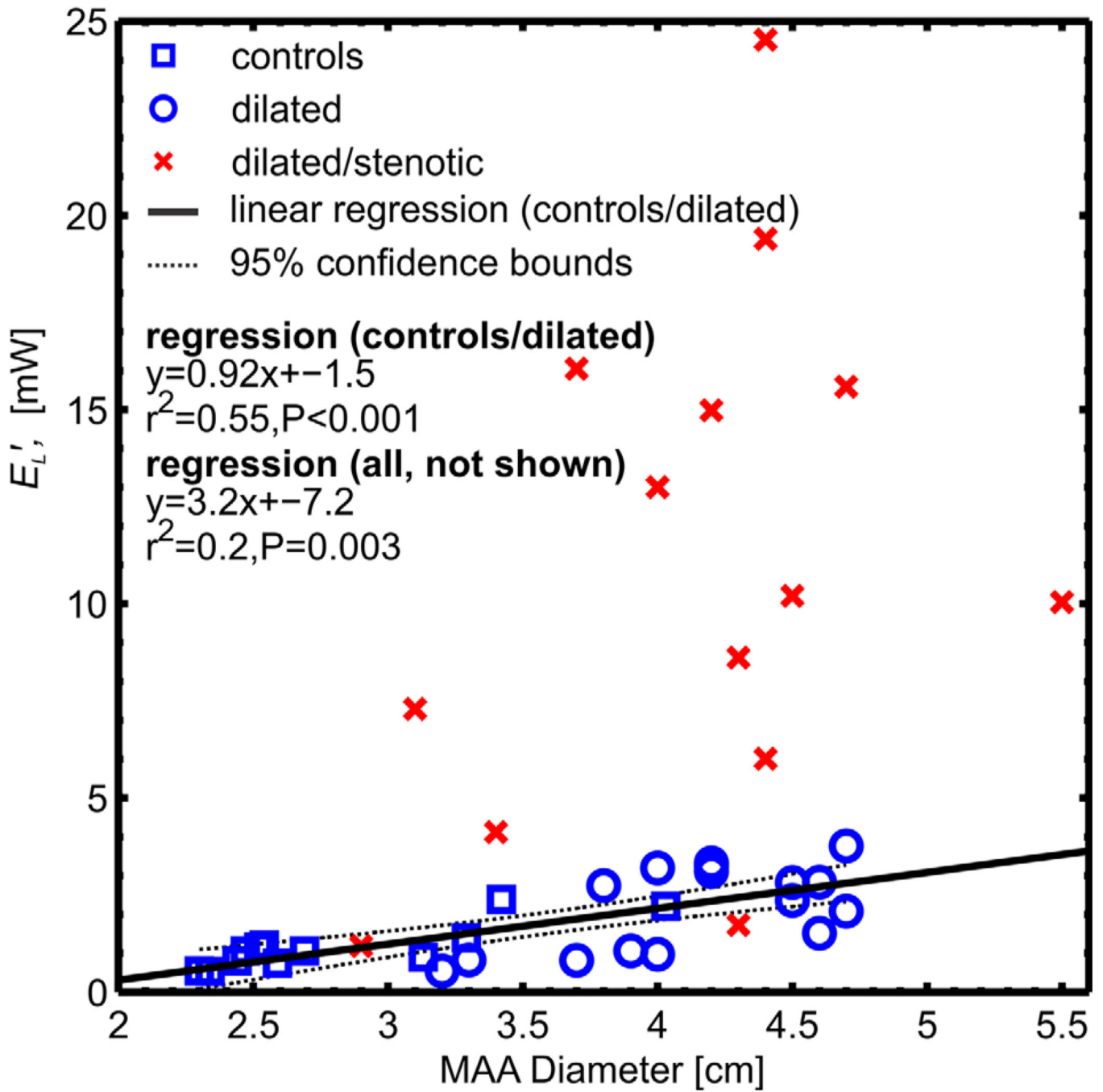
Fig. 6.
Ascending aortic energy loss plotted as a function of mid-ascending aorta (MAA) diameter. A moderate correlation ($r^2=0.55$, $P<0.001$) between energy loss and aortic dilatation was found for the control and dilation-only patient cohort (solid line). No correlation was found in the dilated/stenotic patients due to influence of the aortic valve inflow/outflow geometry on energy loss.

Table 1

Subject Demographics.

	Control	Dilation-only	Dilated/Stenotic	P
n	12	16	14	
Age	37±10	52±8	46±15	0.14
MAA (cm)	2.8±0.5	4.1±0.5	4.1±0.7	0.99
AS (n) mild	-	-	3	
moderate	-	-	5	
severe	-	-	6	
BAV	-	5	7	

MAA: mid-ascending aorta diameter; AS: aortic stenosis; BAV: bicuspid aortic valve; *P* is significance between dilation-only and dilated/stenotic cohort